Title of Proposal: Conscious Agents and the Subatomic World
Authors: Donald Hoffman, Chetan Prakash, Swapan Chattopadhyay

Summary: Physics and evolution agree: Spacetime is doomed. It is not fundamental reality. Nor are its objects. Recently physicists, observing that spacetime has no operational meaning beyond the Plank scale, have discovered that certain mathematical structures, such as amplituhedra and decorated permutations, are more fundamental than spacetime and quantum theory. Thus, a theory that claims consciousness is, or emerges from, the dynamics of physical objects such as neurons, circuits or quantum systems, ignores the verdict of our best science.

We propose a mathematical model in which "conscious agents" are fundamental and interact via a Markovian dynamics. Some agents create spacetime as an interface whereby they interact. Physics is the projection of agent dynamics onto this interface.

This model is bold and speculative, but informed by recent advances in particle physics and mathematics. To test the model, we propose a computational experiment to show that the dynamics of conscious agents predicts the distribution and dynamics of quarks and gluons at all spatial and temporal scales probed by scattering experiments. At high resolution the proton is a sea of gluons. As resolution declines, a sea of quarks is added. With further decline, three valence quarks also appear, two up quarks and one down.

Description of Hypothesis: It is natural to assume that fundamental reality consists of space, time, and physical objects therein. Indeed, this has been a key assumption of science for centuries, including modern quantum field theory and Einstein's theory of gravity, in which space and time are wed into a single fabric of the universe called spacetime. But these same two theories together tell us that spacetime is doomed: it has no operational meaning beyond the Planck scale, roughly 10^{-33} centimeters and 10^{-43} seconds [1–3]. Spacetime, they reveal, is not a fundamental reality.

But this is no problem for physics. Theoretical investigations of the ways that elementary particles collide and scatter suggest new structures beyond—not merely curled up inside—spacetime and quantum theory. These new structures, such as the amplituhedron and decorated permutations, dramatically simplify the computation of quantum "amplitudes" that describe how particles collide and scatter [3–6].

However these structures beyond spacetime are static. They have no interpretation as arising from a dynamics of entities beyond spacetime. We offer such an interpretation: A scientific theory of dynamical entities utterly beyond, and prior to, spacetime and quantum theory, entities

we call *conscious agents* (CAs) [7, 8]. Informally, each CA is a unit of consciousness. It is not a self. It is not smaller than elementary particles. Indeed, it has no size. Size is a feature of spacetime, whereas CAs exist prior to spacetime, and generate spacetime via projection.

A scientific theory starts with assumptions, statements it takes to be true but does not explain. These assumptions are the only "miracles" allowed by the theory. All other assertions of the theory must follow from the assumptions by logic.

Our theory of CAs starts with two assumptions. (1) There exist conscious experiences, such as the taste of chocolate or the mood of elation. (2) There exist probabilistic relations among experiences, such as a tasting of chocolate triggering a feeling of elation.

We formalize these assumptions shortly, in a mathematical definition of a CA. CAs interact and form a network, the *CAnet*, much as Twitter users interact and form the Twitterverse. We propose that the CAnet underlies, and give rise to, the subjective perception of a physical world and a scientific description of spacetime and matter.

Thus, we propose that consciousness is fundamental and gives rise to spacetime and matter. This reverses standard approaches to the "hard problem" of consciousness, which propose that consciousness is not fundamental and must arise from, or be identical to, certain physical or functional systems [9].

Our approach posits, and must explicate, conscious experiences. These include ordinary experiences, such as the taste of coffee or the smell of a rose, and extraordinary, such as meditative experiences of timelessness and fusion with a universal consciousness. It must also explain elemental physical experiences, such as entropic time, flowing from past to present to future, and the phenomenology of the Standard Model of Particle Physics. Our approach is founded on a single unifying principle and a single building block.

Unifying Principle: Conscious experiences and their relationships are fundamental.

Building Block: The mathematical definition of a conscious agent.

We now discuss that building block. A CA has a set of possible conscious experiences. It lies in a network of other CAs, the CAnet, and has a set of possible actions whereby it can affect the conscious experiences of other agents in the network. The experiences, actions, and network are illustrated in Figure 1 with labelled ovals. A CA also has processes by which it (1) decides how to act, (2) acts on the network, and (3) perceives the response of the network. These processes are illustrated with labelled arrows.

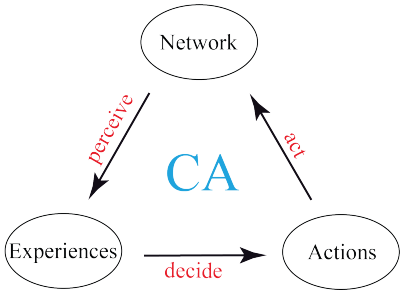

Figure 1. Informal picture of a CA, which acts on a network of other CAs based on its experiences.

So the CAnet is like the Twitterverse, in which there are millions of Twitter users and billions of tweets. The Twitterverse is dynamic. Each user follows certain other users and receives their tweets; this corresponds to the "perceive" map in Figure 1. Each user decides what to retweet and what new tweets to generate; this corresponds to the "decide" map in Figure 1. Each user then sends these tweets out to followers; this corresponds to the "act" map in Figure 1. Received tweets correspond to the "Experiences" in Figure 1.

The CAnet is dynamic. We propose that its dynamics, like the dynamics of many computer networks, is Markovian [10-12]. This means that what the CAnet does next depends only on its state now, and not on prior states. CA dynamics are attractive because they are relatively straightforward, require only finite memory, and are computationally universal: anything computable with neural networks is computable with CAnets. As illustrated in Figure 2, we propose that the CAnet, though beyond spacetime, can project to particles in spacetime via the decorated permutations studied by physicists [3–6].

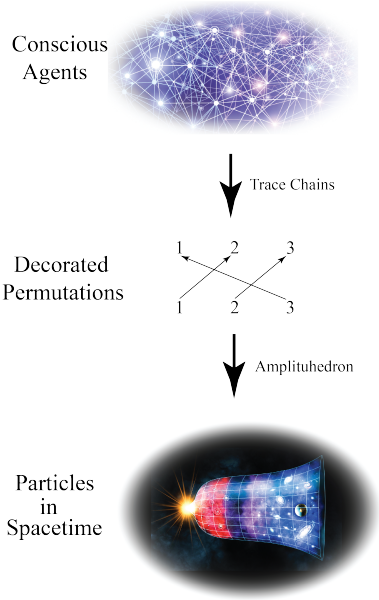

Figure 2. The projection from the CAnet to spacetime via decorated permutations.

The formal theory of a CA models each part of Figure 1 with a mathematical structure. This is illustrated in Figure 3, where the experiences, actions, and network are modeled by *probability spaces*: X, G, and W. The processes of deciding, acting, and perceiving are modeled by *Markovian kernels*: D, A, and P.

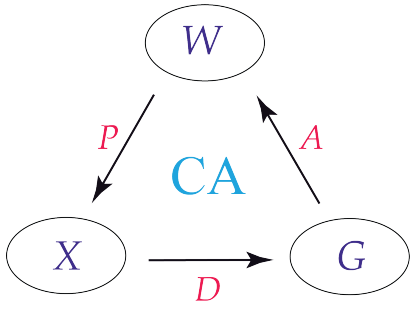

Figure 3. CA diagram.

As an example of a probability space, suppose you toss a coin twice and want to describe what might happen. There are four possible outcomes. For instance, you might get heads on the first toss and tails on the second. Call that outcome *HT*. Or you might get heads on both tosses: *HH*. Then the set of possible outcomes is $\{HH, HT, TH, TT\}$. You might be interested in the probability of certain events, such as the event that you get at least one heads. That would happen if the outcome was in the set $\{HH, HT, TH\}$. So a probability space just lists the possible outcomes, and the interesting events. For CAs, the outcomes are specific conscious experiences, such the taste of coffee, or the feeling of elation. An interesting event might be the experience of coffee followed by elation.

As an example of a Markovian kernel, suppose that you like dessert but want to watch your weight. So if you have dessert today, the chance is only 1 in 3 that you will eat dessert tomorrow; but if you don't have dessert today, the chance is 3 in 4 that you will eat dessert tomorrow. We can write this in a table, as shown in Figure 3. The numbers in each row sum to 1.

		Tomorrow: No Dessert	Tomorrow: Dessert
Today	No Dessert	1/4	3/4
	Dessert	2/3	1/3

Figure 3. Probability of eating dessert.

Mathematicians simplify this table, writing it as a matrix with two rows and two columns:

$$\begin{bmatrix} 1/4 & 3/4 \\ 2/3 & 1/3 \end{bmatrix} \tag{1}$$

This matrix is an example of a Markovian kernel. To model a conscious agent network as complex as the Twitterverse, the matrices for D, A, and P would needs millions of rows and columns. These matrices let us study the dynamics of the CAnet: what experiences are trending, and which CAs are big influencers.

To simplify the study of the conscious experiences of CAs and their long-term behaviors, it helps to multiply the D, A, and P matrices together to create a "qualia matrix" Q:

$$Q = DAP. \tag{2}$$

Here the term *quale* is short for "conscious experience;" its plural is *qualia*. The qualia matrix of a CA answers a question: If my current quale is this (say, the color red) what is the probability that my next quale will be that (say, the color green)?

Indeed, suppose a CA has only two qualia: red and green. Let x be the probability that the next quale is green, given that the current quale is red:

$$x = p(\text{green} \,|\, \text{red}). \tag{3}$$

Let y be the probability that if the CA's current quale is green then its next quale will be red:

$$y = p(\text{red} \,|\, \text{green}). \tag{4}$$

Then the Q matrix of this CA is

$$Q(x, y) = \begin{bmatrix} 1 - x & x \\ y & 1 - y \end{bmatrix}. \tag{5}$$

If $x = 0$, this means that if the CA sees red now it will always see red. If $y = 0$, this means that if the CA sees green now it will always see green. In this case the Q matrix of the CA is the identity matrix:

$$Q(x, y) = \begin{bmatrix} 1 & 0 \\ 0 & 1 \end{bmatrix}. \tag{6}$$

If $x = 1$, this means that if the CA sees red now it will next see green. If $y = 0$, this means that if the CA sees green now it will next see red. In this case the Q matrix of the CA is the NOT matrix:

$$Q(x, y) = \begin{bmatrix} 0 & 1 \\ 1 & 0 \end{bmatrix}. \tag{7}$$

Of course, these are not the only possible values of x and y. Each can take any real value between 0 and 1. So the set of all possible Q matrices for such a CA comprise a unit square that we call the Markov polytope M_2, as shown in Figure 4. It turns out that the collection of all possible matrices for a CA with n qualia is an $n(n-1)$-dimensional polytope in n^n-dimensional real space that we call the Markov polytope M_n. For example, M_3 is a 6-dimensional object sitting in 9-dimensional real space.

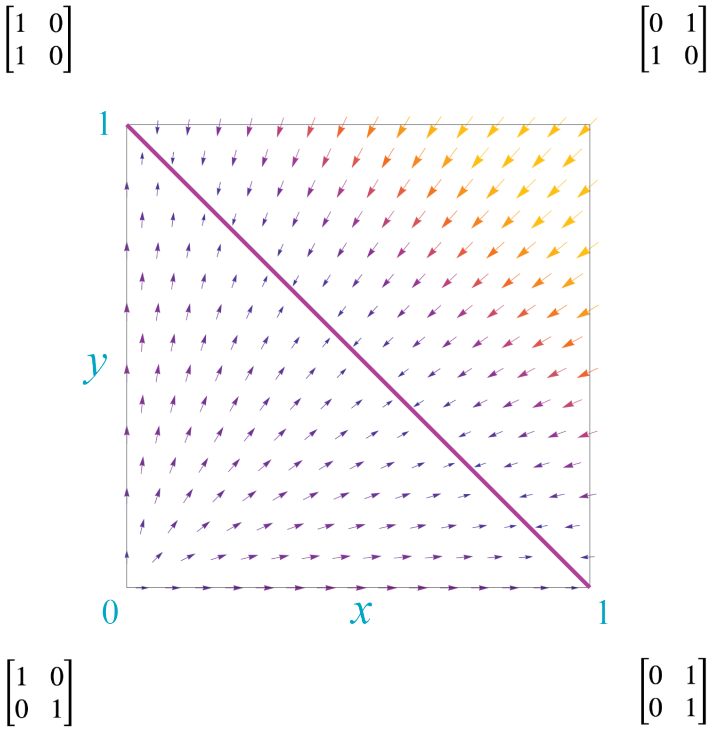

Figure 4. The Markov polytope M_2. Each point of the square represents a possible Q matrix for a CA that has just two qualia. The matrix corresponding to each vertex of the square is explicitly shown.

We can think of this agent as being a combination of two simpler CAs. One CA sees only red and has a matrix, say Q_1; the other CA sees only green and has a matrix Q_2. Then M_2 describes all the interactions whereby the simpler CAs can combine to create the CA with Q. And we can think of Q_1 and Q_2 as two different projections of Q.

Each kernel Q (other than the identity) has a unique combination of colors that it leaves unchanged. We can represent a combination of colors by a probability measure

$$\mu = [\alpha \quad 1-\alpha],\ 0 \leq \alpha \leq 1, \tag{8}$$

where α is the proportion of red and $1-\alpha$ is the proportion of green. The measure μ is *stationary* for the kernel Q if

$$\mu Q = \mu.^{1} \tag{9}$$

The matrix Q gives the probabilities for what this agent will see in the next step. So the matrix $QQ = Q^2$ tells us the probabilities for what it will see in two steps. The difference between Q^2 and Q is a matrix, $Q^2 - Q$, that tells us the difference between the two-step and one-step probabilities. It lets us see the direction of "matrix flows" through M_2, as illustrated in Figure 4 by the little arrows, or vectors [13]. If $Q^2 = Q$, so that the probabilities for one step and two steps are identical, then the flow stops, and the matrix Q is "stationary." The stationary matrices in M_2 are the identity matrix and the matrices along the purple diagonal illustrated in Figure 4; the flow vectors below this diagonal flow up to it, and those above this diagonal flow down to it. Mathematically, this corresponds to the matrices below the diagonal having positive determinants, those above the diagonal having negative determinants, and those along the diagonal having 0 determinants.

The stationary kernels on the purple diagonal lie on the line $y = 1 - x$. Along this line, the matrices can be written as:

$$Q(x,y) = \begin{bmatrix} 1-x & x \\ y & 1-y \end{bmatrix} = \begin{bmatrix} 1-x & x \\ 1-x & x \end{bmatrix}. \tag{10}$$

Thus, when kernels reach this line of stationary kernels, they drop from rank 2 to rank 1, i.e., they go from being a function of two parameters to becoming a function of just one parameter, say

$$\alpha = x = 1 - y. \tag{11}$$

Such a Q is a combination of the agent that sees only red (Q_0 in the left corner of Fig. 5) and the one that sees only green (Q_1 in the right). So we can think of this drop of rank as signaling the fusion of Q_0 and Q_1 into a single agent, Q_α, with a single new quale labelled α. There is a one-parameter family, indeed a unit 1-simplex, of newly-created fused agents, Q_α, each with its own new quale, α, as illustrated in Figure 5.

---

[1] We are using the matrix product of linear algebra.

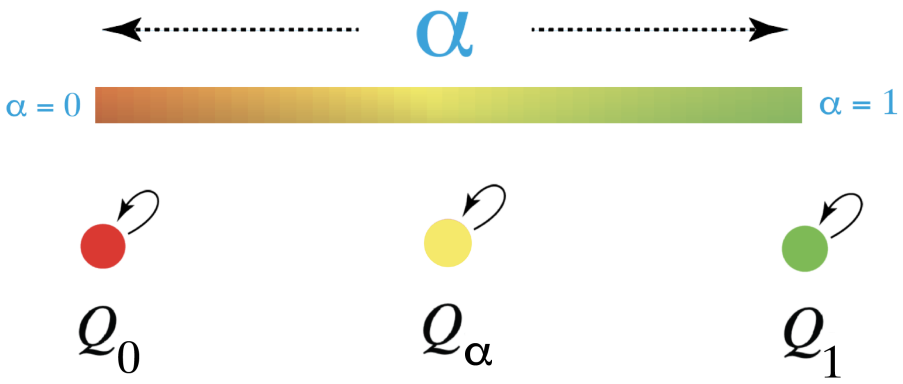

Figure 5. The unit 1-simplex of fusions for two conscious agents. Q_0 only sees red, as indicated by the arrow emerging from and returning to the red dot. Similarly, Q_1 only sees green. The newly created agent, Q_α, only sees the quale α. In this example, $\alpha \approx 0.5$ and the corresponding quale is depicted as yellow, which is what humans see for a roughly 50/50 additive-color mixture of red and green lights. If n conscious agents interact, their possible fusions form a unit $(n-1)$ -simplex (e.g., a triangle in dimension 3).

Any collection of agents is itself an agent. Thus, there is ultimately one agent. A similar stance has been advocated by the physicist Erwin Schrödinger in his essay "Mind and Matter" [14]. However, if we start with a countable infinity, $\aleph_0$, of agents, then the number of possible combinations and fusions is $2^{\aleph_0}$, which is a larger infinity, $\aleph_1$. Then the number of possible new combinations of these $\aleph_1$ agents is yet a larger infinity, $\aleph_2$ and so on endlessly through Cantor's hierarchy of infinities [15]. So the exploration of consciousness through its possible combinations and fusions appears to be endless. For this reason, a theory of consciousness cannot start with a theory of the "Ultimate One Consciousness."

Viewed this way, the smaller units are projections of the One. However, since we cannot start with the One we can, as a first approximation, just start with an agent having a sufficiently large Q kernel. If this agent can perceive n different qualia, then Q is an $n \times n$ Markovian matrix. For any subset, A, of these n qualia we can create a sub-agent by projecting the *trace chain* of the Markovian dynamics of the larger agent on A to get an agent with state space A and kernel Q_A [11, 16].

We can think of a trace chain as arising by running the dynamics of the big chain, and keeping track only of each time it enters one of the states in the subset of the trace. We then use these time-stamped entries to compute the probabilities of transition from one state to another within the subset. For example, consider the 3×3 qualia kernel

$$Q = \begin{bmatrix} 0 & .3 & .7 \\ .4 & 0 & .6 \\ .2 & .8 & 0 \end{bmatrix}. \tag{16}$$

This kernel describes a dynamics on three qualia, say red, green, and blue.[2] We can project this dynamics onto its first and second qualia, red and green, as shown in Figure 6a, or onto its first and third qualia, red and blue, as shown in Figure 6b, or onto its second and third qualia, green and blue, as shown in Figure 6c. The resulting 2×2 qualia kernels are all different.

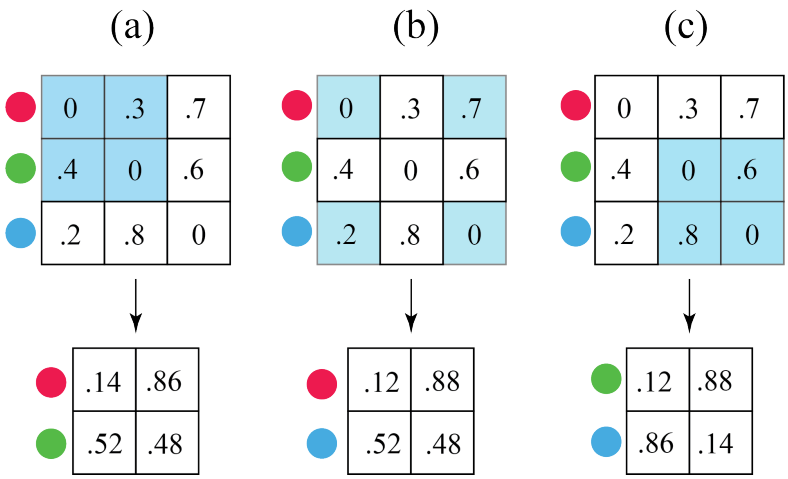

Figure 6. Trace chains.

Thus a trace chain is the projection of the original chain onto a subset of states. We can think of different subsets of states as different "spatial windows" through which the original chain is perceived. As we discuss later, to model data in particle physics we will find it useful to view the *infinite* sequence of steps of a trace chain through *finite* "temporal windows." We will refer to these as "sampled" trace chains.

Another matrix, Q', that can generate the same trace chains as in Figure 9 is

$$Q' = \begin{bmatrix} .14 & .86 & 0 & 0 & 0 & 0 \\ .52 & .48 & 0 & 0 & 0 & 0 \\ 0 & 0 & .12 & .88 & 0 & 0 \\ 0 & 0 & .52 & .48 & 0 & 0 \\ 0 & 0 & 0 & 0 & .12 & .88 \\ 0 & 0 & 0 & 0 & .86 & .14 \end{bmatrix}. \tag{17}$$

[2] We chose Q to have 0's along the diagonal because, as we discuss later, this type of kernel may model "confinement" of particles.

Q' is a Markov chain on six states, one state for each row of the matrix. In this case, the trace of Q' on its first two qualia matches the trace in Figure 6a, the trace on its next two qualia matches Figure 6b, and the trace on its last two qualia matches Figure 6c.

A key difference between Q and Q' is their *communicating classes*: Q has one communicating class and Q' has three. Intuitively, a communicating class is a set of states that "talk" to each other: start at any state in the class and you eventually arrive, with positive probability, at any other state in the class.[3] A communicating class is *recurrent* if there is no escape: if the chain enters the class, it never leaves. Otherwise the class is *transient*.

The three communicating classes in Q' are highlighted in Figure 7. The first class, highlighted in red, contains states 1 and 2. If the chain is in state 1, it stays in state 1 with probability .14 and goes to state 2 with probability .86. If the chain is in state 2, it stays there with probability .52 and goes to state 1 with probability .48. Thus, if the chain starts in states 1 or 2, it will forever go back and forth between those states. So states 1 and 2 form a recurrent communicating class. Similarly, states 3 and 4, highlighted in green, form a communicating class, as do states 5 and 6, highlighted in blue. Mutual communication is an equivalence relation, so the different communicating classes of a given kernel have no overlap and together constitute the whole state space.

$$Q' = \begin{bmatrix} .14 & .86 & 0 & 0 & 0 & 0 \\ .52 & .48 & 0 & 0 & 0 & 0 \\ 0 & 0 & .12 & .88 & 0 & 0 \\ 0 & 0 & .52 & .48 & 0 & 0 \\ 0 & 0 & 0 & 0 & .12 & .88 \\ 0 & 0 & 0 & 0 & .86 & .14 \end{bmatrix}$$

Figure 7. The three communicating classes of Q'.

We discussed communicating classes at length because they are central for projecting the dynamics of CAs down to spacetime and particle dynamics. As we discuss later, physicists discovered to their surprise that decorated permutations invariantly characterize the physical content of scattering amplitudes for particles in spacetime. We proved that Markov chains project canonically to decorated permutations, and thus onto particle scattering [13]. Specifically, decorated permutations classify Markov chains by their recurrent communicating classes [13]. That is why recurrent communicating classes are central to the projection of consciousness into spacetime. By "projection" we mean a dramatic simplification of the more complex dynamics of CAs.

---

[3] For a formal definition of communicating class, see [12].

This leads to the following precise hypotheses:

(1) Each elementary particle of the Standard Model of physics—each boson, lepton, and quark—is a projection of a recurrent communicating class and its Markovian kernel that arise in samplings of trace chains of CAs.
(2) Properties of a free particle—spin, mass, energy and momentum—are projections of properties of the kernel of its recurrent communicating class: e.g., periodicity, entropy rates, hitting times, and stationary distributions.
(3) Each projection is perceivable by some CA via a window, of some finite number of steps, in which the agent observes the corresponding trace chain.
(4) The projection perceived by a CA is, as noted above, a discrete sampling of a trace chain of the larger dynamics onto the states of that CA.
(5) The particles perceived by a CA depend on its subset of states and the number of steps in the window of its trace.
(6) Larger subsets of states and smaller windows of sampling seem, under simulations, to favor periodic perceptions, which we conjecture project to massless particles.

Relevance of Hypothesis to Call: Physicalist science is undeniably successful. Its major theories, such as quantum field theory, general relativity, and evolution by natural selection, transform our world view, explain a plethora of phenomena, and inform breakthroughs in technology. These theories assume that spacetime and its objects are fundamental reality.

The call asks: Could a non-physicalist framework better explain the full range of phenomena? We answer yes. But to do so, a non-physicalist framework must explain everything that physicalist science explains. So the new framework requires, at a minimum, the theoretical precision and mathematical rigor of physicalist theories.

Then it must go further. It must explain what physicalist science does not. It must predict precise new phenomena. It cannot simply offer anomalies or point to shortcomings of physicalism. It must predict precise new phenomena, making novel and numerically precise predictions. And it must do so using new fundamental principles, stated with mathematical precision, that *explain* any anomalies of physicalist theory and remedy its shortcomings: It cannot simply point out such anomalies and shortcomings. Neither the Michelson-Morley experiment nor the anomaly of black-body radiation supplanted Newtonian physics. Quantum theory and relativity did.

We propose a single unifying principle: conscious experiences and their relationships are fundamental. We propose a mathematically precise statement of this principle: the theory of CAs. This theory has one building block: the definition of a CA.

This theory leads to a rich Markovian dynamics of CAs. Critically, this dynamics is utterly beyond spacetime and beyond quantum theory. CAs do not emerge from any physical dynamics

within spacetime. Instead spacetime, with its microphysical particles and macroscopic objects, emerges from the dynamics of CAs. They emerge by projection, that is, by a dramatic simplification of the more complex, yet more unified, dynamics of CAs.

This projection involves two components: trace chains and decorated permutations. A trace chain arises when a smaller CA observes the dynamics of a larger CA in which it is embedded. In this embedding, the possible conscious experiences of the smaller CA are a subset of the conscious experiences of the larger CA. The richer dynamics of the larger CA projects down, via a trace operation, to a dynamics on the experiences of the smaller CA.

This dynamics of the smaller CA depends, statistically, on the specific subset of experiences and specific number of dynamical steps used to compute the trace. In consequence, the dynamics perceived by the smaller CA can differ profoundly from the larger dynamics. In particular, they can differ entirely in their communicating classes.

This is critical. As we discuss in the next section, the communicating classes of a Markov chain completely determine its representation as a decorated permutation. Moreover, physicists have discovered that decorated permutations beyond spacetime determine the characteristics of particle scattering within spacetime. Thus the theory of CAs makes a key prediction: particles in spacetime are not an insight into fundamental reality; they are an artifact of a perceptual projection.

This turns the spacetime reductionist paradigm of physicalism on its head. According to spacetime reductionism, as one probes smaller and smaller regions of spacetime one finds more and more fundamental laws of nature and elements of reality. On this view, microphysical particles—bosons, leptons, and quarks—are fundamental elements of reality. This reductionism motivates most current theories of consciousness, which attempt to show how consciousness emerges from the dynamics of brains, or microtubules, or computer circuits—a dynamics which itself emerges from an even more fundamental dynamics of microphysical particles. This attempt is pointless if the particles themselves are merely artifacts of perception, not fundamental elements of reality.

Thus our hypothesis of CAs entails that spacetime, elementary particles, and physical objects composed of elementary particles are not fundamental reality. Instead, they appear and disappear within the phenomenology of CAs, in a manner that has a precise mathematical statement and can be tested against existing data in scattering experiments at high-energy particle colliders. In particular, brains and neurons do not exist when they are not perceived. Thus brains have no causal powers. They create none of our behaviors and none of our conscious experiences. Subjective phenomenological awareness is not an emergent brain property. Indeed, brains emerge cognitively in phenomenological awareness.

Could a non-physicalist framework better explain the full range of phenomena, including human phenomenology? In principle, yes, because spacetime is doomed: it is not fundamental reality,

and therefore *nor are its particles*. But in practice, much work remains to be done. We outline next steps in our proposed experiment: projecting the Markovian dynamics of CAs down to the spacetime dynamics of elementary particles.

Why project to elementary particles? Why not look instead for a direct connection to brain dynamics, where we have clear evidence for neural correlates of conscious experiences?

For theories proposing that spacetime and its objects are fundamental, and that consciousness emerges from complex physical dynamics, it makes sense to focus on brain dynamics. But physics tell us that spacetime and its objects are not fundamental. So we propose that spacetime and quantum theory emerge from the dynamics of CAs, not vice versa. To test this proposal, we must start as simply as possible: with elementary particles, not complex brains having billions of neurons and trillions of synapses. Physics tell us that the basic properties of elementary particles are intimately linked with the structure of spacetime itself. To study how the dynamics of CAs projects down to elementary particles is to study how the structure of spacetime itself emerges.

So the choice to connect with particle physics is strategic. It is the simplest and most direct route to show that a non-physicalist theory of CAs, not a physicalist theory of spacetime and objects, can better explain the full range of phenomena. That is not to say the projection to particles is simple. As our experimental proposal shows, it is anything but simple. But it is an essential first step. Once it is taken, we can then tackle bigger projects, such as chemistry, biochemistry, and eventually neuroscience and neural correlates of consciousness.

Experiment Proposed: We propose a computational experiment. Its purpose is to answer the following question: Can CAs model the distribution and dynamics of quarks and gluons?

Quarks and gluons are elementary particles in the Standard Model of physics. Figure 8 illustrates where they reside in nature. Macroscopic matter, such as water, is composed of molecules, such as the water molecule H_2O. Molecules are composed of atoms, such as two hydrogens and one oxygen for H_2O. Atoms have a small nucleus, surrounded by negatively charged electrons. The nucleus is composed of neutrons and positively charged protons. Inside neutrons and protons are quarks and gluons.

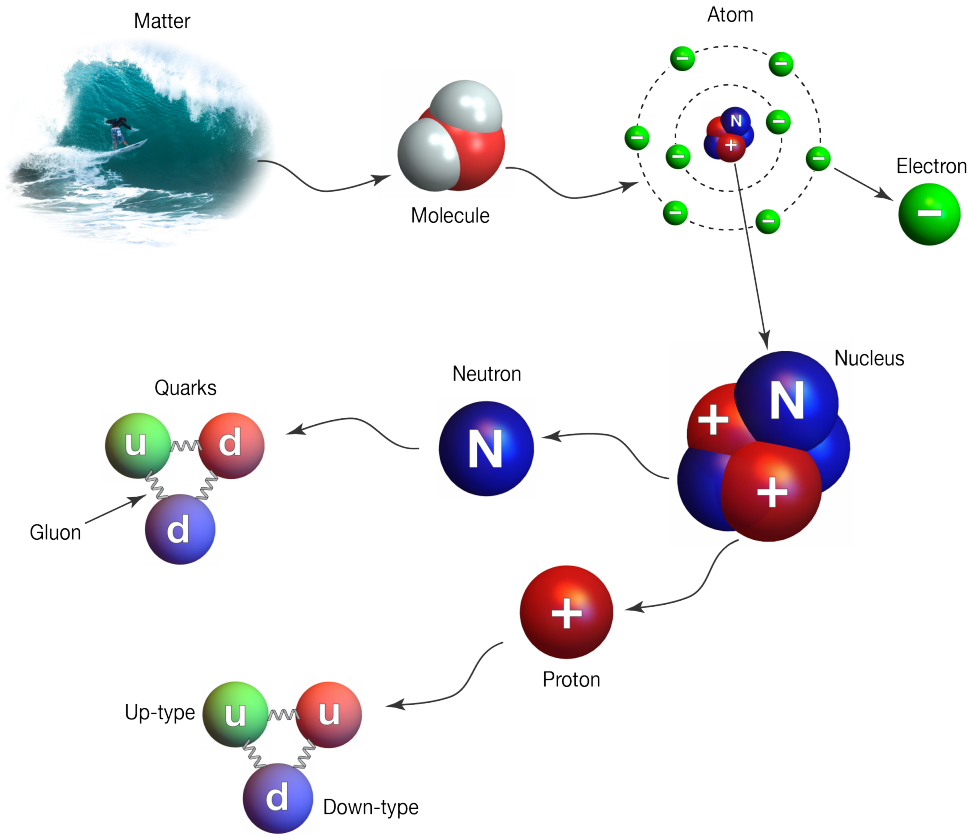

Figure 8. Where quarks and gluons fit within nature. The strong "color" force, mediated by gluons, tethers quarks into neutrons and protons and adheres neutrons and protons into nuclei. Quantum chromodynamics, or QCD, is the current best theory for this process [17].

Powerful cameras, using electrons rather than light, have taken pictures inside of protons. The number of quarks and gluons you find there depends on the resolution and shutter speed of the camera. Figure 9 illustrates the effects of shutter speed, which physicists call "Bjorken *x*."

At fast shutter speeds, the proton is dominated by an ocean of gluons. Gluons are bosons. They are massless, so they always move at the speed of light. A gluon can rupture into more gluons, and two gluons can fuse back into a single gluon.

At medium shutter speeds, a gluon can split into a quark and its antiquark, which is a particle of antimatter. This happens with such frequency that the proton seems to contain a sea of six kinds of quarks.

At slow shutter speeds, three main quarks appear, two "up" quarks and one "down" quark, held together inside the proton by gluons. These are called "valence" quarks. Occasionally a "charm" quark may also appear [19].

So far we have just discussed shutter speed. Experiments have also varied the spatial resolution, which physicists call "Q^2." At fast shutter speeds, as one increases the spatial resolution even more gluons appear. At medium shutter speeds, the sea of quarks gets denser, but the ocean of gluons gets denser at an even faster rate. At slow shutter speeds, the three main quarks become clearer, and the gluons and sea quarks get denser (an informal overview is [20]; technical papers and data are [21-23]; a helpful visualization is [24]).

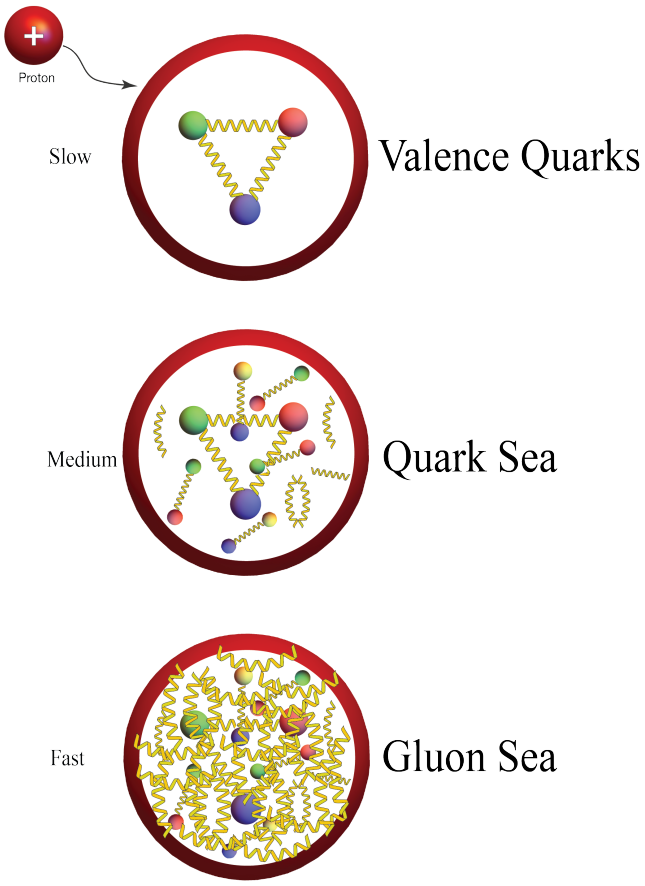

Figure 9. Effects of shutter speed on the quarks and gluons found in a proton. Quarks are represented by colored spheres and gluons by golden springs.

So far we have described the key findings informally. More formally, these data are called the "one-dimensional momentum fractions" or "longitudinal momentum fractions" of quarks and gluons at various values of Bjorken x and Q^2, and have been gathered from "deep inelastic scattering" (DIS), which involves colliding electrons with charged protons at such a high energy that the protons are destroyed [21, 25, 26].

It is these momentum fractions that are the first target of this computational experiment. We want to find a specific class of Markovian dynamics of conscious agents beyond spacetime, and a specific set of projections of that dynamics onto spacetime, that precisely matches the one-dimensional momentum fractions of quarks and gluons at all values of Bjorken x and Q^2 that

have been measured. An example of such data is shown in Figure 10, where "parton" means any particle constituent of the proton.

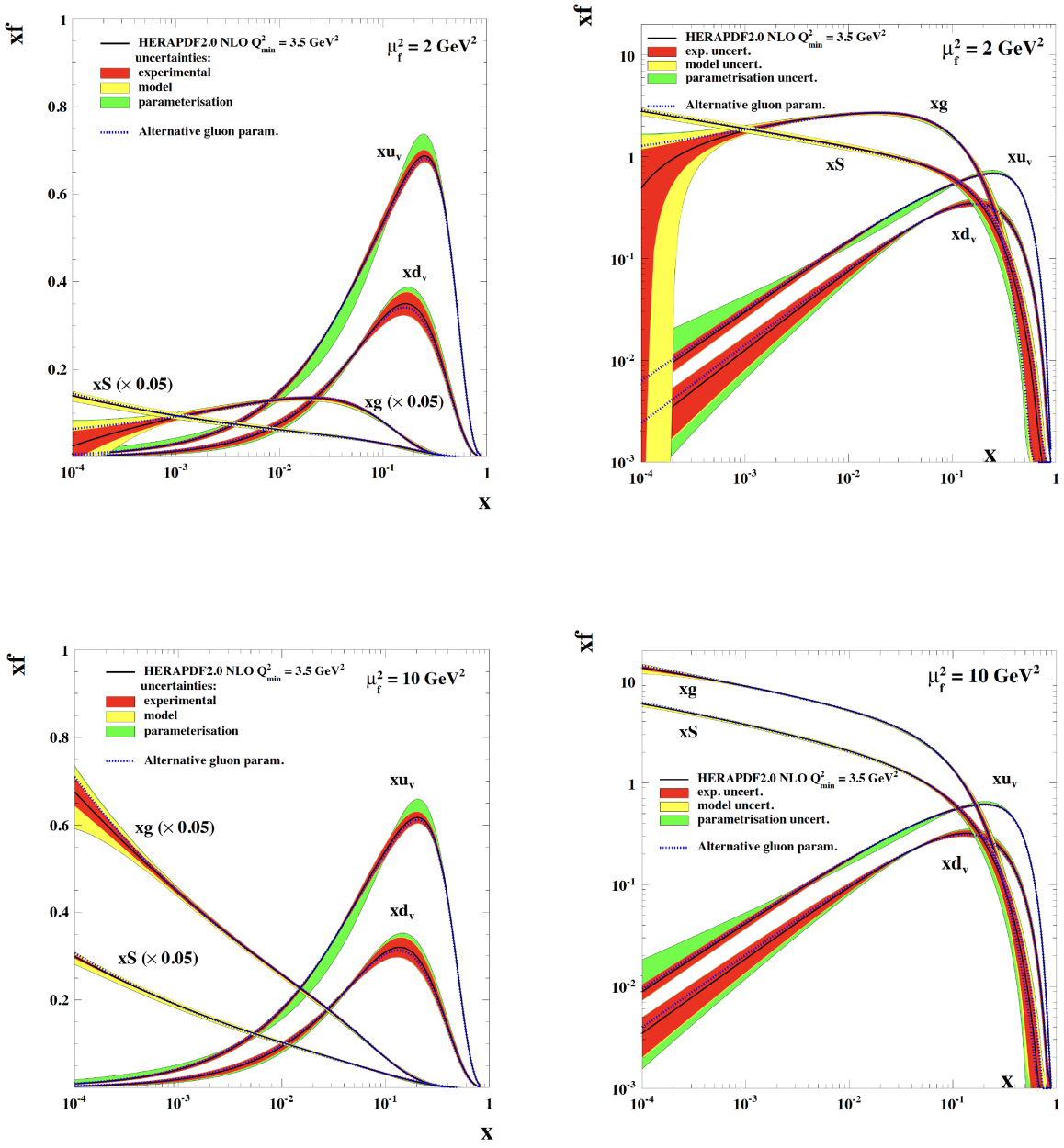

Figure 10. Parton distribution functions. Plots show particle density as a function of Bjorken x. The particles are valence up quarks (xu_v) and down quarks (xd_v), sea quarks (xS), and gluons (xg). Data is combined from the H1 and ZEUS detectors at the HERA particle accelerator in Hamburg. In the two plots on the left the xS and xg curves are scaled down by 1/20. Image credit: Figure 3.1 of [18].

Then we want to use this dynamics of conscious agents to predict the three-dimensional position and momentum distributions for quarks and gluons that experimental physicists plan to study

using a technique called "semi-inclusive deep-inelastic scattering" (SIDIS) on a proposed Electron Ion Collider (EIC).

Then we want to compare the predictions of this conscious agent dynamics *beyond* spacetime with those of "Lattice-QCD," discrete simulations of quantum chromodynamics *within* spacetime, which use a four-dimensional Euclidean spacetime [26]. For instance, how are the spins of sea quarks and gluons distributed within a proton, and how do they contribute to the overall spin of the proton? How do sea quarks and gluons contribute to the overall mass of the proton? These are some of questions we want our computational experiment to answer.

Now we turn to constructing the experiment itself. We first describe, at top level, its key steps. Then we unpack its details. So, at top level, here is what we must do:

1. Find a large and appropriate "master" Markovian matrix.
2. Compute a large number of "sampled" trace chains of the master matrix, systematically varying the number of states and steps in the sample.
3. Identify in each sampled trace chain its Markovian matrix.
4. Find each recurrent communicating class, and its Markovian submatrix, in each sampled matrix. (Free particles in spacetime are expected to be projections of these.)
5. Find any "partite sets" in each sampled matrix. (Confined particles in spacetime are expected to be projections of these.)
6. For the Markovian submatrix of each recurrent communicating class, compute its key properties: the entropy rate (expected to project to mass), the number of states (expected to project to energy), and the action of the submatrix on the "pseudoscalar" (expected to project to spin).
7. Project the recurrent communicating classes and partite sets of each sample Markovian matrix onto decorated permutations.
8. Use these decorated permutations, and the key properties of the recurrent communicating classes, to compute scattering amplitudes in spacetime.
9. Compare the predicted scattering with empirical data from particle colliders.

We now unpack this. From now on, we will freely use the term "particle" for the trace chains and their matrices. This does not imply that the "particle" so identified projects to a known particle in spacetime. Indeed, an object of the proposed experiment is to recognize those particles that are known to current physics, and others that are not. We start with a simple example. For our master matrix we reuse

$$Q = \begin{bmatrix} 0 & .3 & .7 \\ .4 & 0 & .6 \\ .2 & .8 & 0 \end{bmatrix}. \tag{18}$$

Recall that the trace chains of Q on two-state subsets have the 2 x 2 Markovian matrices shown in Figure 11.

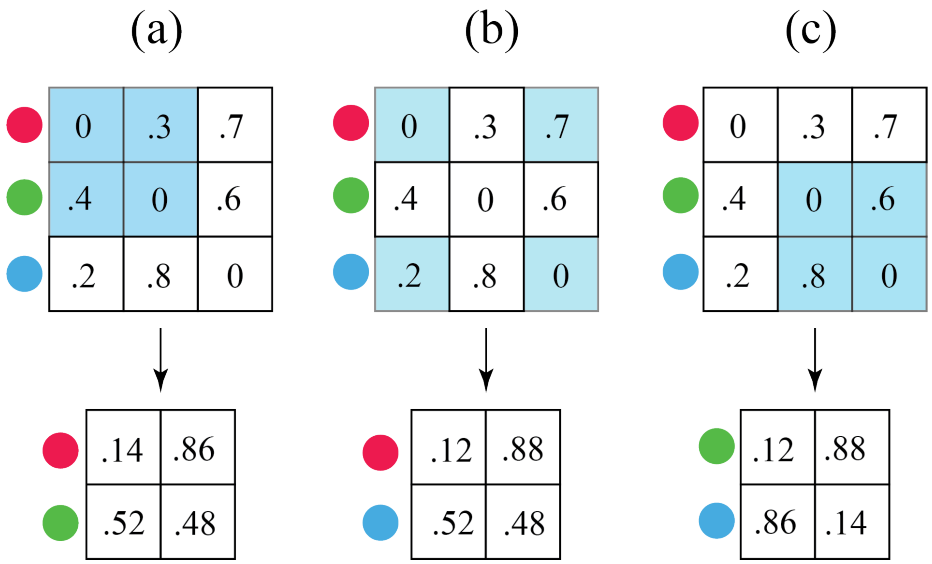

Figure 11. Trace chains of Q.

In particular, note that the trace matrix on the red and green states, states 1 and 2, is

$$Q_{12} = \begin{bmatrix} .14 & .86 \\ .52 & .48 \end{bmatrix}. \tag{19}$$

So now let's compute "sampled" trace chains on the red and green states. To do this, we first use Q to randomly generate a specific sequence, call it $S_{1,2,3}$, of the states 1, 2, 3, where state 1 is red, 2 is green, and 3 is blue. Every run will be different; but an example is

$$S_{1,2,3} = 1, 3, 2, 1, 3, 2, 3, 1, 3, 1, 2, 3, 2, 3, 1, 2, 3, 2, 3, 2, 1, \ldots, \tag{20}$$

From $S_{1,2,3}$ we can create sampled trace chains on states 1 and 2 as follows. First, delete all 3's. This leaves the sequence

$$S_{1,2} = 1, 2, 1, 2, 1, 1, 2, 2, 1, 2, 2, 2, 1, \ldots \tag{21}$$

Then choose a step window. Let's start with a window of three steps. We partition $S_{1,2}$ into the groups

$$S^3_{1,2} = (1, 2, 1), (2, 1, 1),(2, 2, 1), (2, 2, 2), \ldots \tag{22}$$

Now we use each group to create a Markovian matrix that we will call a "sampled matrix." The first group, (1, 2, 1) starts with a transition from state 1 to state 2, then has a transition from state to 2 to state 1. It has no other transitions. So this corresponds to the sampled matrix

$$S^3_{1,2}(1) = \begin{bmatrix} 0 & 1 \\ 1 & 0 \end{bmatrix}. \tag{23}$$

The second group, (2,1,1), starts with a transition from state 2 to state 1, then has a transition from state to 1 to state 1. It has no other transitions. So this corresponds to the sampled matrix

$$S^3_{1,2}(2) = \begin{bmatrix} 1 & 0 \\ 1 & 0 \end{bmatrix}. \tag{24}$$

The third group, (2, 2, 1), starts with a transition from state 2 to state 2, then has a transition from state to 2 to state 1. It has no other transitions. So this corresponds to the sampled matrix

$$S^3_{1,2}(3) = \begin{bmatrix} 0 & 0 \\ .5 & .5 \end{bmatrix}, \tag{25}$$

which is not Markovian.

The fourth group, (2, 2, 2), has two transitions from state 2 to state 2, It has no other transitions. So this corresponds to the sampled matrix

$$S^3_{1,2}(4) = \begin{bmatrix} 0 & 0 \\ 0 & 1 \end{bmatrix}, \tag{26}$$

which can be thought of as a 1 x 1 sampled matrix taking the value 1 on the state 2.

We see three important facts from these four sampled matrices. First, even though all groups have the same number of steps, the sampled matrices they create can and do differ. Second, the entries in these sampled matrices are dominated by 1's and 0's, even though the original matrix Q has no 1's or 0's. Third, the pattern of entries in these sampled matrices little resembles the pattern in the true trace matrix Q_{12}.

All three facts are due to the step size, which is too small to collect enough data to create sampled matrices that closely approximate the true trace matrix Q_{12}. The second and third properties of these sampled matrices are primarily artifacts of the small step size.

If we choose a larger step window of, say, 6 steps, then the first group is (1, 2, 1, 2, 1, 1), which corresponds to the Markovian matrix

$$S^6_{1,2}(1) = \begin{bmatrix} 1/3 & 2/3 \\ 1 & 0 \end{bmatrix}. \tag{27}$$

This still has 1's and 0's and little resembles Q_{12}.

If we increase the step window to 13 steps, then the first group is (1, 2, 1, 2, 1, 1, 2, 2, 1, 2, 2, 2, 1), which corresponds to the Markovian matrix

$$S_{1,2}^{13}(1) = \begin{bmatrix} .20 & .80 \\ .57 & .43 \end{bmatrix}. \tag{28}$$

Finally we have a step window large enough for the sampled matrix to roughly approximate Q_{12}.

Now in this example the master matrix Q is tiny, only three rows and three columns. For our computational experiment to have a chance at properly modeling the momentum fractions of quarks and gluons in the proton, we will need to start with a master matrix that is much larger, perhaps thousands or millions of rows and columns. But we can still expect the sampled matrices to exhibit the same artifacts of step size. In particular, with smaller step sizes, the sampled matrices will be dominated by 1's and 0's. As the size of the master matrix increases, the range of step sizes that lead to sampled matrices dominated by 1's and 0's will also increase.

This is encouraging. We propose that particles with zero mass are projections of communicating classes with zero entropy rate, and such communicating classes have Markovian matrices whose entries are only 0's and 1's. Henceforth we refer to such classes and matrices as "zero mass." So we predict that at small temporal windows, i.e., at small Bjorken x, we should see an ocean of massless particles simply as an artifact of small step sizes in the sampling of the master matrix. This prediction is born out. Physicists find, at small Bjorken x, an ocean of gluons, which are indeed massless particles.

Why should we posit this connection between zero mass and zero entropy rate? Intuitively, the more internal interactions something has, the greater will be its inertia to outside influence: its "inertial mass." Similarly, the more connections a given state of a communicating class has with other states, the more influence it has with other states. If a state has only one connection, then its row in the Markovian kernel is all 0's except for a single 1, and so the entropy of its row is 0. The more connections a state has, i.e., the more nonzero entries it has in its row, the greater its entropy will tend to be. We define the entropy rate of a communicating class to be a weighted sum of the entropies of its rows, where the weighting is the stationary measure of the Markovian kernel of the communicating class [27].

Figure 12 plots the entropy rate for each Markovian matrix in the Markov polytope M_2. The maximum entropy rate in M_2 is 1. The maximum entropy rate for matrices in the Markov polytope M_n is $\log_2 n$. Thus enormous matrices are required to get large masses. For instance, the maximum mass for Markovian matrices of dimension $10^{552} \times 10^{552}$ is about 1834, which is

roughly the proton-electron mass ratio. Now 10^{552} is a lot of elementary conscious agents. To compare, the number of particles in the observable universe is roughly 10^{80}.

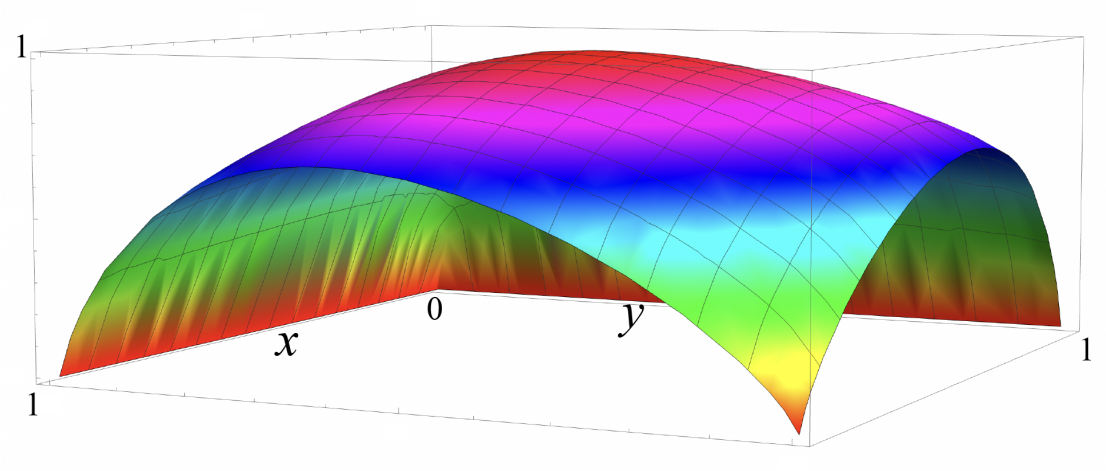

Figure 12. Plot of the entropy rates for all 2×2 Markovian matrices.

If each row of the Markovian matrix for a communicating class has all 0's except for a single 1 then its entropy rate, and its mass, is zero. This entails that a massless communicating class is periodic, since every state in the class can be reached from any other state, and all entries in its Markovian kernel are 0 or 1. The period of the class is the number of states in the class. This suggests a link between the energy of a massless particle and the period of the communicating class that projects to the particle.

Inspired by special relativity, we propose that properties of communicating classes are related to particle mass and momentum as follows: a particle that is a projection of a communicating class with n states has a momentum n and a mass equal to the entropy rate, H, of the class. This entails that a massless particle is a projection of a periodic communicating class and has energy n; a massive particle is a projection of an aperiodic communicating class and has an energy given by $\sqrt{n^2 + H^2}$. (Here we use "natural" units, in which $c = \hbar = 1$, where c is the speed of light and $\hbar$ is the reduced Planck constant.)

Suppose we start with a large master matrix that has a single communicating class, and that we choose a large subset of its states to sample. Then as the number of steps in the sample increases we expect two consequences. First, as we saw in our simple example, if the initial matrix is aperiodic the larger step size leads to a sample matrix with many entries that are not 0 or 1 (see the matrix in equation (28)), and that therefore has a nonzero entropy rate. Second, the size of the communicating classes within it will also tend to increase. These two consequences entail that the corresponding particle masses are growing.

Again this is encouraging. At small values of Bjorken x, i.e., at fast shutter speeds, the interior of the proton appears to be an ocean of massless gluons. But as one decreases the shutter speed, the

proton appears to acquire a sea of quarks whose masses increase as the shutter speed decreases. Eventually, with low enough shutter speeds, three large valence quarks appear. This trend emerges, qualitatively, from sampled trace chains of conscious agent dynamics, and is an artifact of the sampling process itself. A goal of this computational experiment is to show that it can emerge not just qualitatively, but in precise correspondence with empirical data from particle colliders.

Varying the spatial resolution of sampled traces is the analog of varying Q^2 in particle colliders. In addition to systematically varying the step size of the sampled traces, the experiment must also systematically vary the number of states of the sampled traces. If we think of the step size as the "temporal resolution" of the sampled trace, then we might think of the number of states as its "spatial resolution." The highest spatial resolution would be a trace on all states of the master matrix. But then one could choose to trace on every other state, every third state, every 100th state, and so on. For a Markovian dynamics on n states (n conscious experiences) there are $2^n - 1$ windows of states and countless windows of steps. Thus this is a rich area for computational experiments.

The qualitative effect of spatial resolution is clear. If the step size is small, so that the sampled matrix has mostly 0's and 1's and thus mostly massless communicating classes, then increasing the number of states of the trace will exaggerate this, creating more 0's and 1's and thus more massless communicating classes. In short, the sampling artifacts will increase. This exaggeration of sampling artifacts will occur at all step sizes. As the step size gets very large, this exaggeration of artifacts will lessen and the sampled matrix will approach the correct trace matrix.

This qualitatively matches the effects of varying Q^2 in deep inelastic scattering experiments on protons. The goal of this computational experiment is a quantitative match: Find a master matrix and sampled traces that precisely match the one-dimensional momentum fractions of quarks and gluons at all values of Bjorken x and Q^2 that have been measured.

We propose that *free* particles are projections of communicating classes. But particles are not always free. Particles can be bound together, such as when an electron and proton bind to form a hydrogen atom. The strengths of binding vary across combinations of particles. The binding of quarks is so strong that they are said to be "confined." Quarks are never free particles at normal temperatures, but are always grouped together into hadrons, such as protons, neutrons, and pions. This property of quarks is called "quark confinement." Only if the temperature exceeds the Hagedorn temperature, about 1.7×10^{12} K, do quarks become free, forming a quark-gluon plasma.

So the relationship between particles can vary on a continuum from free to bound to confined. We can model this variation using Markovian kernels, as illustrated in Figure 13. The first kernel has two communicating classes, one highlighted in green and one in blue. There is no interaction between the two classes, and so this models free particles. The mass of the green class is the entropy rate of states 1 and 2; the mass of the blue is the entropy rate of states 3 and 4.

The second kernel in the figure has just one communicating class, which consists of all four states of the kernel. However, this kernel is almost identical to the kernel above it, with just the addition of small interaction terms, highlighted in red. So this models the case where the two particles are weakly bound and represent, together, a compound particle. The binding strength between particles can be varied from weak to strong, depending on the size of the interaction terms. We can quantify this by dividing the entropy rate of states 1 and 2 into two parts: the *kinetic* entropy rate (H_k), which is the part colored green and corresponds to the mass of the particle, and the *potential* entropy rate (H_p), corresponding to the binding mass in red. Similarly for states 3 and 4 in blue. We will say, suggestively, that a particle is "free" if $H_p = 0$, "bound" if $0 < H_p < H_k$, and "confined" otherwise.

With stronger binding, particles are confined, as shown in the third kernel. In this kernel the dominant terms are the interaction terms, highlighted in green and blue. In this case the entropy rate of states 1 and 2 is primarily binding mass, as is the entropy rate of states 3 and 4.

$$Q = \begin{bmatrix} .14 & .86 & 0 & 0 \\ .52 & .48 & 0 & 0 \\ 0 & 0 & .12 & .88 \\ 0 & 0 & .52 & .48 \end{bmatrix} \text{ FREE}$$

$$Q = \begin{bmatrix} .14 & .85 & 0 & .01 \\ .52 & .48 & 0 & 0 \\ 0 & 0 & .12 & .88 \\ .01 & 0 & .51 & .48 \end{bmatrix} \text{ BOUND}$$

$$Q = \begin{bmatrix} 0 & 0 & .14 & .86 \\ 0 & 0 & .52 & .48 \\ .12 & .88 & 0 & 0 \\ .52 & .48 & 0 & 0 \end{bmatrix} \text{ CONFINED}$$

Figure 13. Markov chains for free, bound, and confined particles.

The mass of the three valence quarks of a proton constitute about 2% of the mass of the proton. We can model this by placing 98% of the entropy rate in the bindings.

To each Markovian matrix we can associate a graph, called its *diagram*, as illustrated in Figure 14. Nodes of the graph denote states of the matrix and the weighted directed-edges denote transition probabilities. Figure 14 shows the diagram associated to each matrix of Figure 13. Red, green, blue and yellow nodes denote, respectively, states 1, 2, 3, and 4 of the matrix.

Of particular interest is the diagram of the confined matrix. Note that the pair consisting of the red and green nodes connects only to the the pair consisting of yellow and blue nodes, and vice versa. The red and green nodes have no connections between them, and the blue and yellow nodes have no connections between them. This is an example of a "bipartite graph" with two "partite sets." The first partite set contains the red and green nodes, and the second partite set contains the blue and yellow nodes. This example happens to be a "complete" bipartite graph, in which every node of one partite set connects with every node of each other partite set. This illustrates an important connection between particle confinement and partite sets.

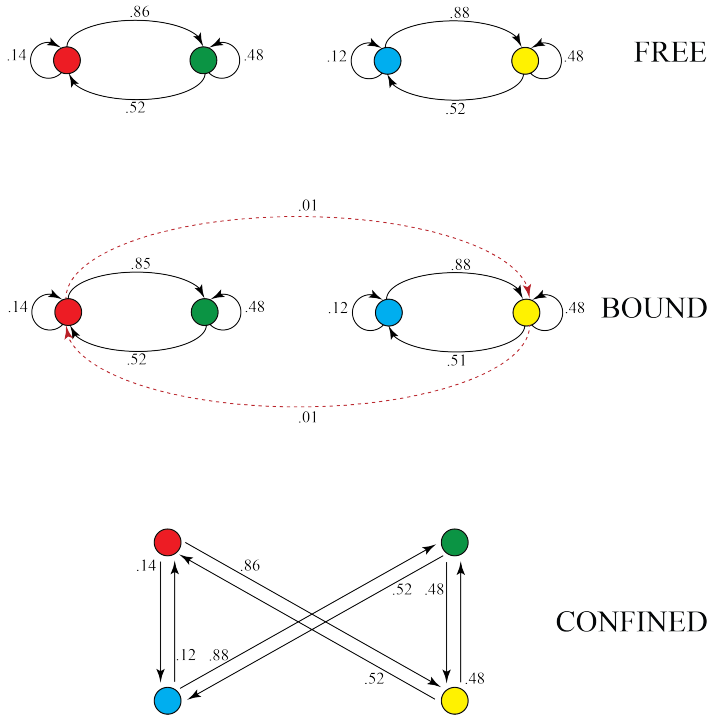

Figure 14. Graph representations for the qualia kernels of Figure 13.

Graphs can also be tripartite, having three distinct partite sets. These may be critical for our computational experiment, since the proton, at large values of Bjorken *x*, consists primarily of three valence quarks that are confined within the proton. The proton itself would be modeled by a Markovian matrix with a single communicating class, and the quarks confined within the proton would be modeled by having the states of the communicating class be divided into three partite sets. This suggests that for a computational experiment to successfully model the experimentally-determined momentum distributions of quarks and gluons at all values of Q^2 and Bjorken *x,* the master matrix from which all sampled trace matrices are derived may itself need to have a tripartite graph. We shall see. That is one of the points of doing the computational experiment. It may turn out that the master matrix only needs to have three sets of nodes that are strongly bound rather than completely confined.

Spin is an essential aspect of our main computational experiment, whose goal is to model momentum distributions of quarks and gluons in protons; quarks and protons have spin ½, and gluons have spin 1. We have proposed a correspondence between specific properties of a communicating class and the mass, energy, and momentum of a spacetime particle that is its projection. We now briefly discuss what property of a communicating class could project to spin. We restrict attention to the spin values (0, ½ , 1), and leave discussion of the values 3/2 and 2 to later work.

First recall that the outer product of n arbitrary vectors, $v_1, \ldots, v_n$, can be visualized as any n-dimensional shape with volume $\|v_1 \wedge \ldots \wedge v_n\|$ (e.g., [28]). We give two illustrations in Figure 15, using a parallelepiped and an ellipsoid.

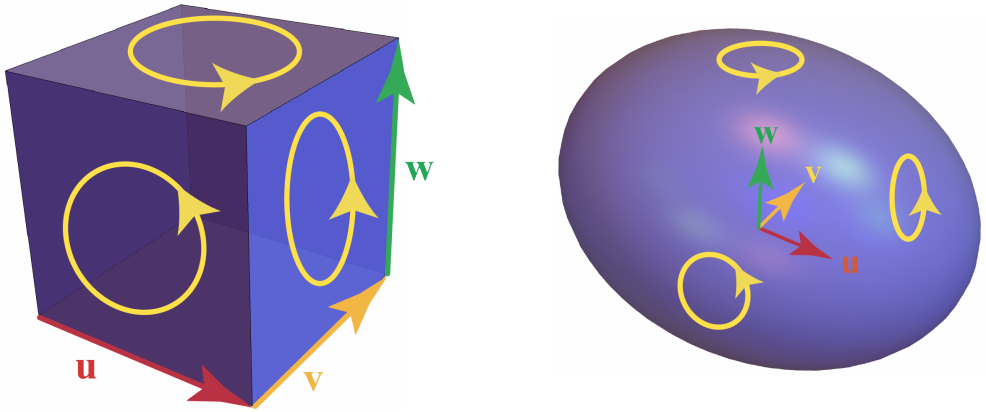

Figure 15. Graphic representations of the outer product of three vectors, **u**, **v**, **w**. The circles with arrows indicate the orientations of the pairwise outer products.

Let C be a communicating class with n states and Markovian kernel Q. Let $e_1, \ldots, e_n$ be an orthonormal set of unit vectors in $\mathfrak{R}^n$, and let $I = e_1 \wedge \ldots \wedge e_n$ be their outer product. In geometric algebra, I is called a "pseudoscalar." We can think of I as a hypercube of dimension n and volume 1.

For any vector v, thought of as a column matrix, the usual matrix product Qv is again a vector. Now define $Q(I)$ to be the outer product $Q(I) = Qe_1 \wedge \ldots \wedge Qe_n$. We will call $Q(I)$ the "C-spin" of the communicating class C. Intuitively, Q distorts the hypercube I into a parallelepiped, $Q(I)$. $Q(I)$ has a magnitude $V = \det Q$ that satisfies $-1 \leq V \leq 1$, because Q is a Markovian matrix. The C-spin number is 1 if $|V| = 1$, 0 if $|V| = 0$, and ½ otherwise. If $Q(I)$ has a major axis, then it is the axis of C-spin. For example, consider a communicating class with Markovian matrix

$$Q = \begin{bmatrix} .240898 & .386297 & .372804 \\ .787596 & .0787703 & .133634 \\ .728801 & .236085 & .0351143 \end{bmatrix}, \tag{29}$$

we find that the basis vectors, e_1, e_2, e_3, get transformed to new vectors, $Q(e_1), Q(e_2), Q(e_3)$, as follows:

$$\begin{aligned} Q(e_1) &= Q(1,0,0) = (.240898, .787596, .728801) \\ Q(e_2) &= Q(0,1,0) = (.386297, .078770, .236085) \\ Q(e_3) &= Q(0,0,1) = (.372804, .133634, .035114) \end{aligned} \tag{30}$$

Their magnitudes are $\|Q(e_1)\| = 1.09977$, $\|Q(e_2)\| = .459529$, and $\|Q(e_3)\| = .397585$. $Q(e_1)$ has the greatest magnitude, so the unit cube gets transformed to a parallelepiped with major axis $Q(e_1)$, as shown in Figure 16, and $Q(e_1)$ is the axis of C-spin. The volume of this parallelepiped is $V = \det Q = .0679224$, which corresponds to a small C-spin up.

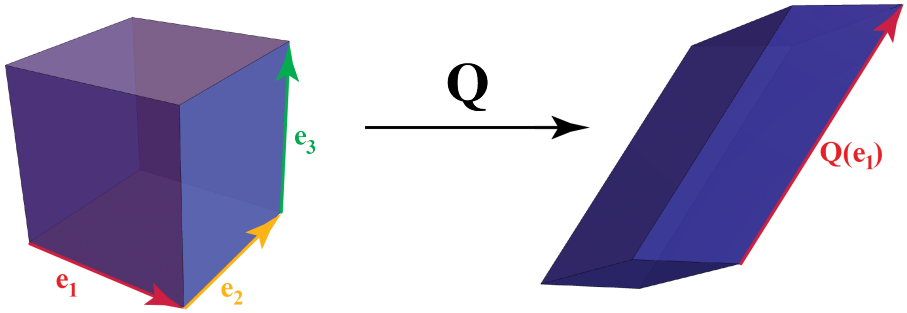

Figure 16. Graphic representation of the C-spin axis of a Markovian kernel Q.

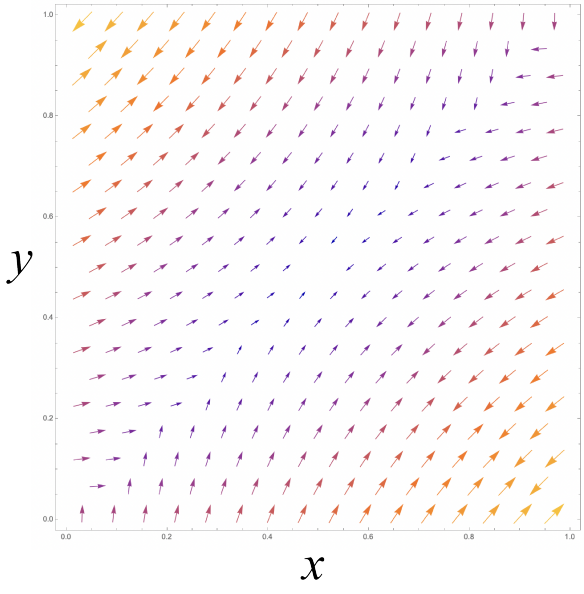

Figure 17. The C-spin axis for each Markovian kernel of M_2 as given by the transformation $Q(I)$.

Figure 17 plots the C-spin axis for each 2×2 Markovian matrix in the Markov polytope M_2. Note that the C-spin along the line $y = x$, which is isomorphic to the "Birkhoff polytope $\mathscr{B}_2$", has magnitude $1 - 2x$ and no preferred axis. The C-spin of matrices in M_2 reverses direction at the line $y = 1 - x$, which is the fusion simplex. The C-spin has magnitude 0, and thus no preferred direction, everywhere within the fusion simplex.

We propose that the spin number (0, ½ , 1) and spin axis of a subatomic particle, p, is the projection into spacetime of the C-spin, $Q(I)$, of its corresponding communicating class. We think of this communicating class as arising from a sampled trace chain, so that the communicating class and the particle to which it projects are both results of an observation, and are not taken as an objective reality independent of observation.

If C is massless (i.e., has zero entropy rate) and has n states, then we can think of $Q(I)$, the C-spin, as a hypercube of dimension n. This hypercube has no preferred direction. Thus the only parameter is its signed volume, which is 1 or -1. We propose that C projects to a massless particle of spin 1 and momentum n. For reasons we now describe, its helicity in the direction of momentum is 1 if n is odd and -1 if n is even.

Suppose C is massless and has n states. If n is even, then its matrix has signed volume -1. A Markovian matrix of even dimensions can approach volume $+1$, but cannot arrive because it disintegrates into smaller communicating classes. If n is odd, then its matrix has signed volume $+1$. A Markovian matrix of odd dimensions can approach volume -1, but cannot arrive because it disintegrates into smaller communicating classes. This subtlety might have physical implications, such as massive bosons and hyperfine structure.

If C is massive and the volume of $Q(I)$ is not 0, then we can think of $Q(I)$, the C-spin, as a parallelepiped with a major-axis. This C-spin projects to a massive particle of spin ½ whose spin axis is the projection of the major axis of the parallelepiped and whose mass is the entropy rate of Q. If the volume of $Q(I)$ is positive the particle has spin up; otherwise it has spin down.

If C is massive and the volume of $Q(I)$ is 0, then the C-spin is 0. The mass of C is the entropy rate of Q.

The sea quarks within the proton are primarily quark and anti-quark pairs generated by gluons. So we must propose how the distinction between matter and antimatter particles arises from Markov polytopes. This is an open question. But we note that the Markov polytope $\mathscr{M}_n$ might be partitioned into two parts, say by its $(n-1)$-dimensional fusion simplex. One part, $\mathscr{M}_n^I$, contains the identity matrix, and the other part, $\mathscr{M}_n^{-I}$, does not. Instead, $\mathscr{M}_n^{-I}$ contains the maximal-derangement vertices.

Perhaps antimatter particles are projections into spacetime of recurrent communicating classes of Markovian kernels in $\mathscr{M}_n^I$, and matter particles are projections into spacetime of recurrent communicating classes of Markovian kernels in $\mathscr{M}_n^{-I}$.

Suppose we now have a large number of sampled trace chains, with their sampled Markovian matrices, communicating classes, partite classes, and key properties. We have systematically varied the number of states and steps in the samples, to cover the range of resolutions and shutter speeds needed to match the empirically determined momentum distributions of quarks and gluons inside the proton at various values of Q^2 and Bjorken x. Our next step is to project these sampled matrices onto decorated permutations.

Why? Because physicists have discovered that decorated permutations—outside of spacetime—together with key properties like mass and spin, allow them to compute all amplitudes for particle scattering processes within spacetime. So if we project our dynamics of conscious agents onto decorated permutations, we can simply use what physicists have already discovered to compute scattering amplitudes. Physicists have already done the hard work. We just need to connect with it. We connect by projecting the dynamics of conscious agents onto decorated permutations.

Intuitively, a permutation is like shuffling a deck of cards. A deck of 52 cards has about 8×10^{67} ways it can be shuffled, and each way is a different permutation. A decorated permutation is a slight generalization of permutations.[4]

Decorated permutations can be represented by diagrams that mathematicians call "plabic graphs" and physicists call "on-shell diagrams" [4, 29]. For instance, for the decorated permutation [3, 4, 5, 6], an on-shell diagram is shown in Figure 18. The numbers to be permuted are arranged around a circle clockwise. To read off the permutation from the diagram, follow the line from a number into the diagram. If the line hits a white dot, turn left. If it hits a black dot, turn right. For instance, the line inward from 1 hits a white dot, so we turn left and hit a black dot, so we turn right and hit a white dot, so we turn left and arrive at 3. Thus, 1 is permuted to 3. Similarly, the line inward from 2 hits a black dot, so we turn right and hit a white dot, so we turn left and hit a black dot, so we turn right and arrive at 4. Thus, 2 is permuted to 4. If we start with 3, we will end up at 1. However, observe that, for the corresponding decorated permutation, we now have to add 4, because $a = 3 > \sigma(a) = 1$, so we end up with $3 \to 5$. Analogously, we find $4 \to 6$.

[4] More precisely, a permutation on the set $\bar{n} := \{1, \ldots, n\}$ is a one-to-one mapping from the set onto itself. We denote permutations by $s = [s(1), s(2), \ldots, s(n)]$. An ordinary permutation, s, can be *decorated* to yield mappings $\sigma : \bar{n} \to \bar{2n} = \{1,\ldots, 2n\}$ in the following ways: for each $a \in \bar{n}$, if $s(a) > a$, set $\sigma(a) = s(a)$; if $s(a) < a$, set $\sigma(a) = s(a) + n$; if $s(a) = a$, set $\sigma(a)$ to be either a or $a + n$.

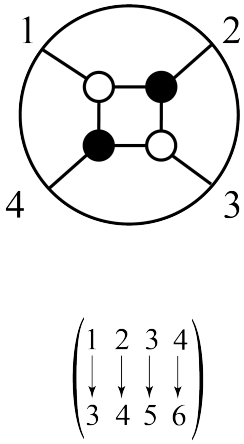

Figure 18. On-shell diagram for the decorated permutation $\sigma = [3,4,5,6]$.

In the other direction, for a given decorated permutation, there are many corresponding on-shell diagrams, of varying complexity. The diagram of relevance to physicists computing scattering amplitudes is a "reduced" diagram. It can be obtained by decomposing the decorated permutation into a minimal sequence of "adjacent" transpositions by a simple algorithm, which can then be used to generate a corresponding on-shell diagram that is reduced [4].

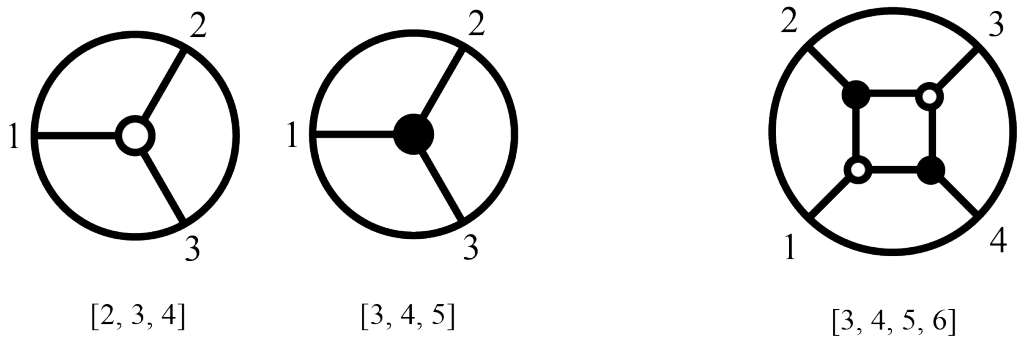

Figure 19. Physicists' scattering amplitudes and decorated permutations for three and four-particle scattering [4].

Figure 19 shows the physically possible scattering diagrams and decorated permutations for three and four-particle scattering. The two decorated permutations for physically possible five-particle scattering are $[3, 4, 5, 6, 7]$ and $[4, 5, 6, 7, 8]$. For six-particle scattering they are $[3, 4, 5, 6, 7, 8]$ and $[4, 5, 6, 7, 8, 9]$.

The map from Markov polytopes via decorated permutations to quantum amplitudes allows us to project the dynamics of CAnets into spacetime physics. Our computational experiment gathers data about this projection for the dynamics of quarks and gluons inside protons. As our experiment learns to match empirical data about up quarks, down quarks and gluons, we will

refine our understanding of the projection of CA dynamics to particle dynamics, and of the genesis of mass, spin, energy, momentum, and antimatter.

Up quarks, down quarks, and gluons are, of course, just a start. The Standard Model of particle physics sports many elementary particles, as shown in Figure 20. There are fermions, including six flavors of quarks and six flavors of leptons, all having spin ½. There are bosons with spin 1, including photons, the Z, two kinds of W, and eight kinds of gluons. Finally, there is the Higgs boson, with spin 0. There is extensive empirical data on these particles, gathered over decades through experiments with particle accelerators [21]. To be taken seriously, the theory of CAs must show how all of this data arises as the projection of CA dynamics.

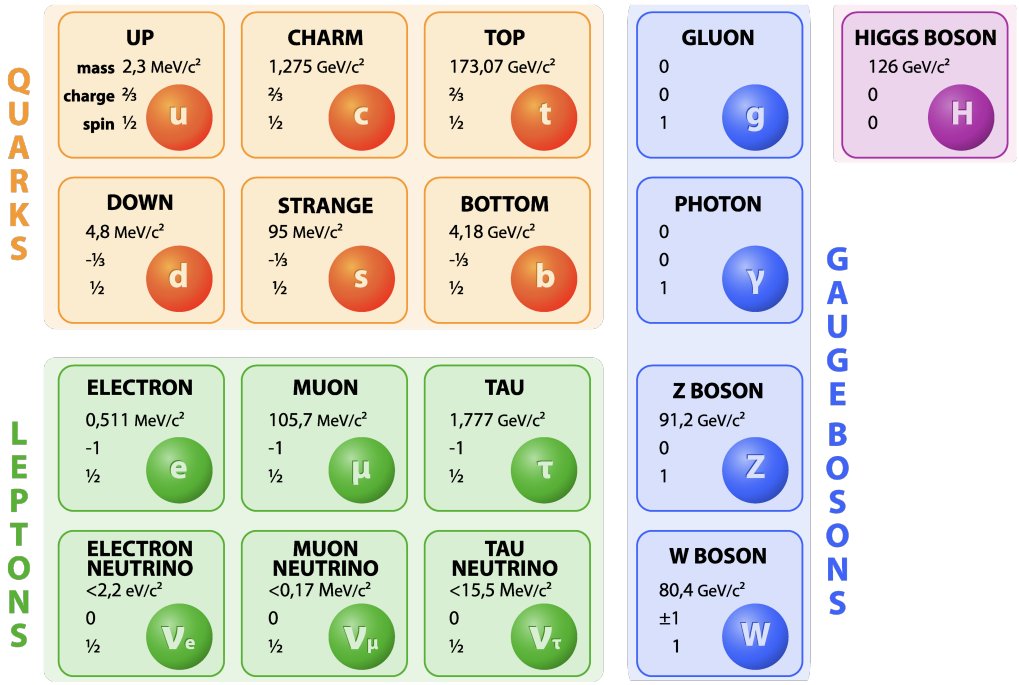

Figure 20. The Standard Model of particle physics.

But the theory of CAs must do more. Many mysteries remain unresolved in The Standard Model, and CAs must explain them. For instance, in The Standard Model the masses of leptons and quarks arise from their interactions with the Higgs field, which is illustrated in Figure 21. But most of the mass and energy in the observable universe is dark. How precisely do CAs give rise to the Higgs field, dark matter, and dark energy? CAs offer promising tools to tackle these problems: entropy rates and sampled trace chains.

For instance, as discussed earlier, trace chains on large numbers of states and small windows of step size tend to produce communicating classes with zero entropy rates. As the windows grow, the entropy rates eventually become nonzero and grow. This provides an avenue to explain why

the Higgs field is zero at high temperatures, and only confers mass when the temperature drops low enough.

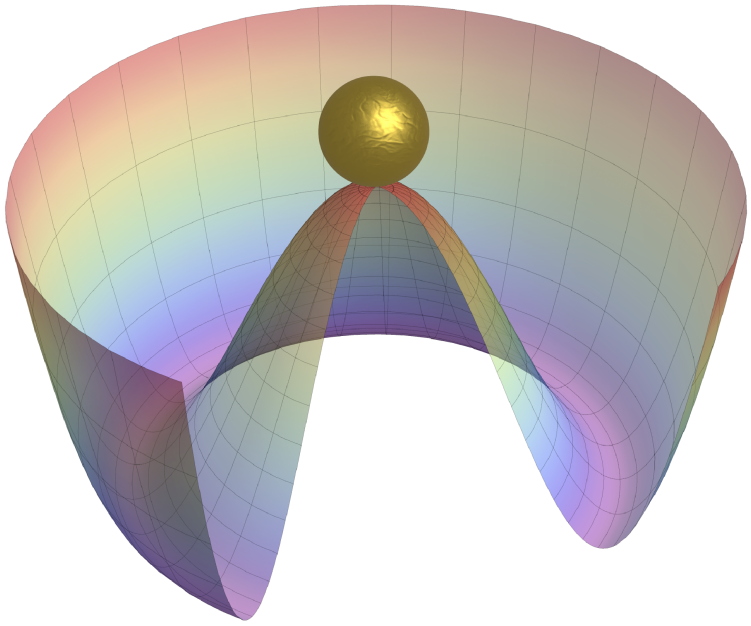

Figure 21. The Higgs Boson of the Standard Model of particle physics sits precariously at the top of the local meta-stable energy-intensive point of the "Mexican-hat" potential of the Higgs scalar field.

Moreover, sampled trace chains allow CAs to model the effects of unobserved "dark" states of CA dynamics that are excluded from the trace or whose traces do not project to known particles. This provides a potential avenue to explain the origin of dark matter.

One mystery of The Standard Model that may dissolve for CAs is the "vacuum catastrophe": the enormous energy density of the vacuum predicted by quantum field theory, the so-called "zero-point" energy, deviates from the tiny measured value, the "cosmological constant," by 50 to 120 orders of magnitude [30]. CAs, whose sampled trace chains have step windows of finite minimum size, will likely avoid the problem.

Another mystery of The Standard Model that may dissolve for CAs is the unitarity problem [31-33]. Quantum theory requires unitary evolution: when particles interact all probabilities sum to 1, so that past determines future and vice versa. But an expanding universe continuously adds new degrees of freedom, in violation of unitarity. The projection of CA theory into spacetime may avoid this problem because CA dynamics is so much richer [13].

One more mystery is the oscillation of neutrinos. As a neutrino travels through space it transmutes identity between "flavors" of electron neutrino, muon neutrino, and tau neutrino, as

illustrated in Figure 22. This may be addressed by CA theory using "weakly periodic" Markovian chains, which asymptotically exhibit periodic oscillations of the kernel and the probability measure on states [10, §6.12]. Oscillations of the kernel may model "flavor" changes, and oscillations of the measure may model mass changes.

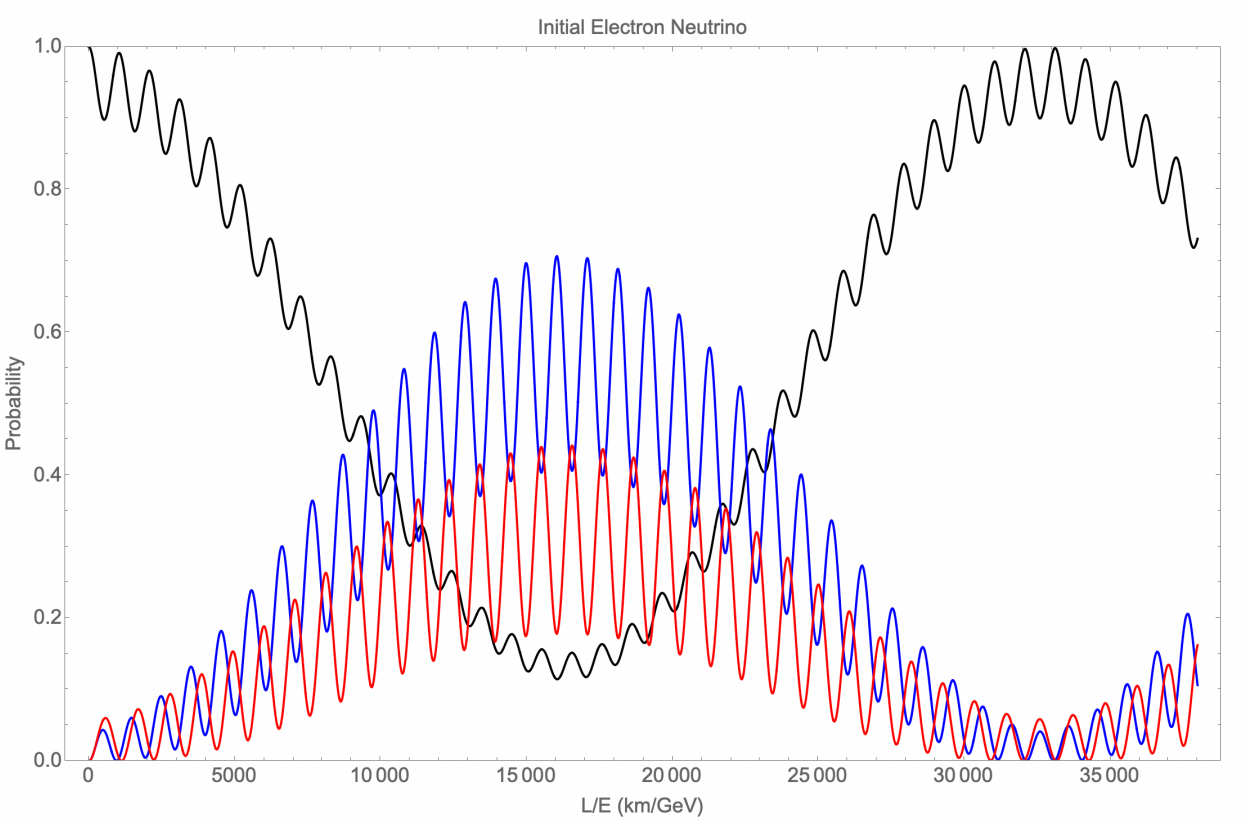

Figure 22. Neutrino oscillations. Image credit: Balázs Meszéna, "Neutrino Oscillations." http://demonstrations.wolfram.com/NeutrinoOscillations/, Wolfram Demonstrations Project.

Future experiments: The computational experiment proposed here explores how the strong force, which dominates inside protons, may arise from a dynamics of conscious agents. Future computational experiments will explore gravity, the weak force, the electromagnetic force, dark matter, and cosmology from the Big Bang to the entropic death of the universe. Our proof-of-concept experiments suggest that sampled trace chains converge to a single communicating class as the step windows of the trace increase in size. This class then gradually increases in entropy until the entire Markovian dynamics drops to rank 1, and effectively disappears. This suggests entropy death at long time scales for the universe.

Our goal is to give the scientific community a reason to take seriously the idea that consciousness is fundamental, that consciousness can be modeled with precise mathematics and make precise experimental predictions, and that the dynamics of consciousness gives rise to spacetime physics via a projection that can be studied precisely.

An experiment whose outcome appears anomalous to current physics will not, by itself, persuade the scientific community that consciousness is fundamental. And for good reason. For science to take consciousness seriously, any new experiment must be grounded in a mathematical theory of consciousness that yields physical science as a special case and, in addition, predicts the anomalous outcome of the new experiment. Only then will mainstream science consider the possibility that consciousness is fundamental, not emergent. And when they do, their genius will be unleashed. We can't wait to read their papers.

The network of CAs offers mathematical form to the central tenet of perennial philosophy: all emerges from One. This tenet appears in spiritual traditions as Indra's net, the body of Christ, Atman is Brahman; in philosophy as a centerpiece of Platonism, renaissance humanism, and the monadology of Leibniz [34]. The latter, with its pre-established harmony of monads, invites modeling as CAs arising from the One via sampled trace chains. Spiritual traditions rightly observe that their teachings may point to truth, but are not truth, just as "coffee" is not the drink. Likewise, scientific theories, including CA theory, only point. Their advantage, however, is that they point more precisely and, in the best case, reveal their necessary limits. This prompts ever new theories that transcend prior limits, in a virtuous cycle that unmasks the poverty of dogmatism and the intelligence of humility.

Acknowledgement: The four images in Figure 10 were obtained courtesy of Prof. Max Klein and Prof. Claire Gwenlan, co-authors of reference [18] cited in the caption.

References

[1] Gross, D. (2005). Einstein and the search for unification. *Current Science*, 89, 2035–2040. https://doi.org/10.1142/9789812772718_0001.

[2] Musser, G. (2016). Spacetime is doomed. In Wuppuluri, S., Ghirardi, G. (Eds), *Space, time and the limits of human understanding*. (New York: Springer). ISBN: 978-3-319-44418-5.

[3] Arkani-Hamed, N. (2019). Spacetime and quantum mechanics: Total positivity and motives. Harvard Lectures. https://www.youtube.com/watch?v=Sn0W_mwA7Q0.

[4] Arkani-Hamed, N., Bourjaily, J., Cachazo, F., Goncharov, A., Postnikov, A., Trnka, J. (2016). *Grassmanian geometry of scattering amplitudes*. (Cambridge, UK: Cambridge University Press). https://doi.org/10.1017/CBO9781316091548.

[5] Arkani-Hamed, N., Huang, T.C., Huang, Y.t. (2021). Scattering amplitudes for all masses and spins. https://arxiv.org/abs/1709.04891v2 [hep-th].

[6] Arkani-Hamed, N., Benincasa, P. (2018). On the emergence of Lorentz invariance and unitarity from the scattering facet of cosmological polytopes. https://arxiv.org/abs/1811.01125v1 [hep-th].

[7] Hoffman, D.D., Prakash, C. (2014). Objects of consciousness. *Frontiers in Psychology*, 5. https://doi.org/10.3389/fpsyg.2014.00577.

[8] Fields, C., Hoffman, D.D., Prakash, C., Singh, M. (2018). Conscious agent networks: Formal analysis and application to cognition. *Cognitive Systems Research*, 47, 186–213. https://doi.org/10.1016/j.cogsys.2017.10.003.

[9] Blackmore, S., Troscianko, E. (2018). *Consciousness: An introduction,* Third Edition. (New York: Routledge).

[10] Gebali, F. (2017). *Analysis of computer networks*. (New York: Springer).

[11] Revuz, D. (1984). *Markov chains*. (Amsterdam: North Holland).

[12] Levin, D., Peres, Y. (2017). *Markov chains and mixing times*, second edition. (Providence, Rhode Island: American Mathematical Society).

[13] Hoffman, D.D., Prakash, C., Prentner, R. (2023). Fusions of consciousness. Entropy, 25, 1, 129. https://doi.org/10.3390/e25010129, https://www.mdpi.com/1099-4300/25/1/129.

[14] Schrödinger, E. (1958). *Mind and matter.* (Cambridge, UK: Cambridge University Press).

[15] nLab authors. Cantor's Theorem. (2022). Available online: https://ncatlab.org/nlab/show/Cantor%27s+theorem.

[16] Bennett, B., Hoffman, D., Prakash, C. (1989). *Observer mechanics: A formal theory of perception*. (New York: Academic Press).

[17] Campbell, J., Huston, J., Krauss, F. (2018). *The black book of quantum chromodynamics*. (Oxford, UK: Oxford University Press).

[18] Agostini, P., et al. (2021). The Large Hadron–Electron Collider at the HL-LHC. *Journal of Physics G: Nuclear and Particle Physics*, 48, 11. https://doi.org/10.1088/1361-6471/abf3ba.

[19] Ball, R. et al. (2022). Evidence for intrinsic charm quarks in the proton. *Nature*, https://doi.org/10.1038/s41586-022-04998-2.

[20] Inside the Proton, the 'Most Complicated Thing You Could Possibly Imagine', (2022). Quanta Magazine, https://www.quantamagazine.org/inside-the-proton-the-most-complicated-thing-imaginable-20221019/.

[21] Workman, R. L. et al. (Particle Data Group). (2022). *Progress of Theoretical and Experimental Physics*, 083C01. https://pdg.lbl.gov/2022/html/computer_read.html.

[22] Donnelly, T. et al. (2017). *Foundations of nuclear and particle physics*. (Cambridge, UK: Cambridge University Press). https://doi.org/10.1017/9781139028264.

[23] National Academies of Sciences, Engineering, and Medicine. (2018). *An Assessment of U.S.-Based Electron-Ion Collider Science*. (Washington, DC: The National Academies Press). https://doi.org/10.17226/25171.

[24] Visualizing the proton. MIT documentary. https://www.youtube.com/watch?v=G-9I0buDi4s

[25] H1 and ZEUS Collaborations, F.D. Aaron et al., JHEP 01, 109 (2010), hep-ex/0911.0884

[26] Lin, H. (2020). Frontiers in lattice nucleon structure. *International Journal of Modern Physics A*, 35, Nos. 11 & 12. DOI: 10.1142/S0217751X20300069.

[27] Cover, T.M., Thomas, J. (2006). *Elements of information theory*, 2nd ed. (Hoboken, NJ: Wiley).

[28] Doran, C., Lassenby, A. (2010). *Geometric algebra for physicists*. (Cambridge, UK: Cambridge University Press).

[29] Postnikov, A., Speyer, D.,Williams, L. (2008). Matching polytopes, toric geometry, and the totally non-negative Grassmannian., arXiv:0706.2501v3.

[30] Adler, R. Casey, B., Jacob, O. (1995). Vacuum catastrophe: An elementary exposition of the cosmological constant problem. *American Journal of Physics*. 63 (7): 620–626. doi:10.1119/1.17850

[31] Cotler, J., Strominger, A. (2022). The universe as a quantum encoder. https://arxiv.org/abs/2201.11658

[32] Dittrich, B., Höhn, P. (2012). Canonical simplicial gravity. *Classical and Quantum Gravity*, 29, 11. DOI 10.1088/0264-9381/29/11/115009.

[33] Wood, C. (2022). Physicists rewrite a quantum rule that clashes with our universe. *Quanta Magazine*, https://www.quantamagazine.org/physicists-rewrite-a-quantum-rule-that-clashes-with-our-universe-20220926/.

[34] Leibniz, G.W. (2005). *Discourse on Metaphysics and The Monadology.* (Mineola, New York: Dover).